

PREPARED FOR SUBMISSION TO JCAP

Conformal Holographic Dark Energy

Mario A. Rodríguez-Meza^a Jorge L. Cervantes-Cota^a Tonatiuh Matos^b

^aDepartamento de Física, Instituto Nacional de Investigaciones Nucleares, Apartado Postal 18-1027, Col. Escandón, Ciudad de México, 11801, México.

^bDepartamento de Física, Centro de Investigación y de Estudios Avanzados del Instituto Politécnico Nacional, Av. Instituto Politécnico Nacional 2508, San Pedro Zacatenco, México 07360, CDMX.

E-mail: marioalberto.rodriguezmeza@inin.gob.mx, jorge.cervantes@inin.gob.mx, tonatiuh.matos@cinvestav.mx

Abstract. Recent results from the DESI collaboration suggest a preference for an evolving dark energy (DE) component rather than a cosmological constant, motivating the exploration of alternative models for the background expansion. These data also reveal tension in the inferred matter density parameter—lower in DESI and higher in Planck—as well as a neutrino mass posterior that approaches the lower bounds permitted by oscillation experiments. In this work, we propose and test a conformal holographic dark energy (CHDE) model in which the DE density depends on a power law of the conformal time, characterized by an exponent (n). This formulation introduces a single additional parameter relative to Λ CDM and reduces to Λ CDM in the limit $n = 0$. We confront the CHDE model with BAO, CMB, and supernova datasets, following the same combinations used by DESI, and perform parameter inference under both flat and non-flat cosmologies. Our analyses show that Λ CDM is not favored as the best-fit model when using CMB data alone or in joint analyses including BAO and SNIa, and it is disfavored at the 4.4σ level for non-flat model and 4.5σ for the flat model. We obtain consistent values of $n \sim -0.28$ to -0.32 with uncertainties less than ± 0.1 across multiple data combinations. Similar to Λ CDM, the CHDE model predicts a lower matter density when employing DESI data instead of Planck data. This, in turn, influences the neutrino mass constraints, yielding values close to the minimal allowed range. Despite these data-set-dependent tensions, both the flat and curved CHDE models remain compatible with neutrino mass constraints from terrestrial experiments and yield posterior distributions that peaks at positive values. This behavior avoids the issue encountered in the Λ CDM model, where the posterior peaks at negative mass values. The CHDE model passes all current observational tests and provide a viable alternative to constant dark energy in light of emerging dynamical evidence.

Keywords: Holographic dark energy, generalized cosmologies, cosmic probes, neutrino mass.

Contents

1	Introduction	1
2	The CHDE model	2
3	Model testing with cosmological data	4
4	Conclusions	10
A	Alternative interpretation of the CHDE model	13
B	Cosmological equations for class	14
C	Full contour plots of the CHDE model	15

1 Introduction

The standard model of cosmology is based on a content of baryons, photons, neutrinos, cold dark matter, and dark energy (DE). Although we do not know the origin of cold dark matter, we have characterized its gravitational effects at different astrophysical and cosmological scales, and it seems consistent with its cold origin, but interesting alternatives have been discussed in the literature such as warm and fuzzy dark matter. On the other hand, we know less about DE, but it is clear that a cosmological constant is the simplest way to account for the cosmic acceleration. For many years, the Λ CDM model has been remarkably successful in explaining a wide range of cosmological observations, including supernova distance measurements, cosmic chronometers, the Cosmic Microwave Background (CMB), and large-scale structure clustering statistics. However, the cosmological constant has recently been called into question by the joint analysis of Baryon Acoustic Oscillations (BAO) performed by the DESI collaboration Year 1 [1–3] and Year 2 [4, 5], DES final BAO [6], and supernovae results: Pantheon+ [7, 8], Union3 [9], and DES Year 5 [10]. Their analysis suggests that the DE responsible for the current epoch of cosmic acceleration is decreasing at present. In any case, the results provide evidence in favor of a dynamical form of dark energy rather than a strictly constant one. Because the origin of this behavior remains unclear, numerous alternative explanations have been proposed. These can be broadly classified into fundamental theoretical models and parametrized phenomenological models.

As far as we know, cosmological data does not reveal DE clustering properties, but it mainly manifests its effect in the background dynamics (apart from the ISW effect). Therefore, when thinking of passing from a cosmological constant to a function, it seems appealing to associate a cosmological function with no clustering properties, or, if any, at very large distances such as horizon scales, and that is why a holographic Universe is accommodated in a natural way. Holographic dark energy (HDE) has been a popular model for years, and different realizations of it have been put forward [11]. Here we discuss a holographic model that depends on the conformal time. However, our model is different from the well-known agreaphic models [11, 12], in which matter conservation is defined apart from the Einstein equations, assumed to be valid. In our case, the cosmological DE function will be explicitly

written in the Einstein equations, so energy conservation demands an interaction between our HDE model and dark matter in particular. Our model has the mathematical properties of a vacuum DE model as the one presented in refs. [13, 14].

On the other hand, recent cosmological measurements of the neutrino mass by the DESI collaboration [4] suggest extremely small values that may conflict with limits established by terrestrial neutrino oscillation experiments. Some DESI data combinations even seem to disfavor both the normal and inverted mass hierarchies, and the preferred values in the statistical analyses tend to lie in unphysical, negative regions [15]. These tensions motivate the exploration of alternative cosmological scenarios. One proposal is to allow spatial curvature to vary, which weakens the constraints and shifts the inferred values toward more physically plausible ones [16]. However, even in this case, the most likely value remains close to zero, indicating that a full resolution of the issue might require analyses that allow for effectively negative neutrino masses. In this context, DE models must be examined to determine whether they can resolve or at least mitigate the tension in the inferred neutrino mass. For example, the $w_0 w_a$ CDM model [17, 18] offers some relief, but it does not fully eliminate the problem once all datasets are considered. We will investigate this question within our proposed model.

This work is organized as follows: In section 2 we present the CHDE model and derive the relevant equations. In section 3 we employ different datasets and free parameters to extract the physical information of the model. Finally, in section 4 we review our results and conclude.

2 The CHDE model

We start with the Einstein equations with a holographic term given by [19]:

$$R^{\mu\nu} - \frac{1}{2}Rg^{\mu\nu} + \mathcal{M}h_c^2g^{\mu\nu} = \kappa^2 T^{\mu\nu}, \quad (2.1)$$

where $\kappa^2 = 8\pi G/c^4$; G is Newton's gravitational constant, $T^{\mu\nu}$ contains the standard matter pieces of the standard cosmological model (baryons, cold dark matter (DM), and relativistic particles), and \mathcal{M} is an holographic function that will depend on the horizon distance and will play the role of a cosmological, dark energy function. One may postulate different holographic functions, see e.g. [11], which typically depend on the physical horizon. But one can also consider the comoving horizon. In a previous work, one of us opted for this option taking $\mathcal{M} \sim \frac{1}{\lambda^2}$, where λ is the cosmological length scale given by $\lambda = \frac{c}{H_0} R_H$, where $R_H = H_0 \int_0^t dt' / a(t')$ is the FRW comoving horizon, where $a(t)$ is the scale factor, t the cosmic time and H_0 the Hubble constant. This model was motivated by its connection to de Proca gravity and the interpretation that it represents a gravitational wave background [20]. We added appendix A, where the main features of that model are explained. Regardless of that interpretation, in the present work we aim at finding out the most favored DE model, letting it be a more general function. Given the form of R_H , it is convenient to present our model in terms of conformal time ($d\eta = dt/a(t)$). Our conformal holographic dark energy (CHDE) is

$$\mathcal{M} = \text{const.} \eta^n, \quad (2.2)$$

where the exponent n is a constant and the *const* is convenient to be defined as *const* = $Q H_0^{n+2}$, with Q an adimensional constant of order one related to the cosmological function evaluated today. The two constants will be determined by fitting observational data.

Note that it is convenient to define $\rho_{\mathcal{M}} = \mathcal{M}/8\pi G$ and therefore

$$\Omega_{\mathcal{M}} = \frac{\rho_{\mathcal{M}}}{\rho_c} = \Omega_{\mathcal{M}}^{(0)} \left(\frac{\eta}{\eta_0} \right)^n, \quad (2.3)$$

where $\Omega_{\mathcal{M}}^{(0)} \equiv \frac{1}{3}Q(H_0\eta_0)^n$ and ρ_c the standard critical density. Eq. (2.3) is our cosmological function, in which the cosmological scale, $\eta_0 \sim H_0^{-1}$ is the comoving scale evaluated at present times; in principle, it can be thought of as a fundamental scale responsible for DE. Assuming a flat FRW background geometry, the gravitational equations (2.1) imply

$$\frac{\mathcal{H}^2}{H_0^2} = \frac{\Omega_b^{(0)}}{a} + \frac{\Omega_\gamma^{(0)}}{a^2} + \Omega_{dm}^{(0)} \frac{\rho_{dm}}{\rho_{dm}^{(0)}} a^2 + \Omega_{\mathcal{M}}^{(0)} a^2 \left(\frac{\eta}{\eta_0} \right)^n, \quad (2.4)$$

where $\mathcal{H} \equiv \frac{a'}{a} = \frac{1}{a} \frac{da}{d\eta}$; we will also consider the curvature that can be added to this equation. Adopting a particular value for n , the CHDE model has the same degrees of freedom as the Λ CDM model. Note that one can recover the Λ CDM model for $n = 0$; $n = -2$ was used in previous works by one of the authors [19, 20]. On the other hand, if there is no interaction between DM and CHDE ($Q = 0$), $\rho_{dm} \sim 1/a^3$, one recovers the Einstein de Sitter Universe. But, in general, matter conservation demands

$$\rho'_{dm} + 3\mathcal{H}\rho_{dm} = -n \frac{\rho_c^{(0)}}{\eta_0} \Omega_{\mathcal{M}}^{(0)} \left(\frac{\eta}{\eta_0} \right)^{n-1}. \quad (2.5)$$

where $\rho_c^{(0)} \equiv 3H_0^2/8\pi G$. This equation specifies the interaction of DM with CHDE, in which one can directly observe that DM is created if $n < 0$, and it is sourced by a time decaying function for $n < 1$. The CHDE is a geometric term, but in analogy to the Λ CDM model, it can be thought of as a perfect fluid, so that the r.h.s. of eq. (2.5) is equal to $-[\rho'_{\mathcal{M}} + 3\mathcal{H}(1 + w_{\mathcal{M}})\rho_{\mathcal{M}}]$, therefore, this equation shows that $w_{\mathcal{M}} = -1$. This can also be seen from eq. (2.1): the relationship between $\rho_{\mathcal{M}}$ and $p_{\mathcal{M}}$ is given similar to the Λ CDM model, $T_{\mathcal{M}}^{\mu\nu} = -\mathcal{M}g^{\mu\nu}/\kappa^2$, from which one can read off the equation of state (EoS) for \mathcal{M} . This deduction is the similar as the presented in references [13, 14].

Since we aim to solve the system of equations (2.4) and (2.5) using `class` [21], we write in appendix B the corresponding `class` equations in which we make use of the conformal and cosmic times as well as the number of e-folds parameter, $N(\equiv \ln a)$. The last term of eq. 2.4 (B.7) decreases in the past for $n > 0$, but diverges for $n < 0$, however in a matter- or radiation-dominated universe, the energy density diverges too as $\rho_{dm} \sim 1/\eta^6$ and $\rho_\gamma \sim 1/\eta^4$, respectively. Thus, the final result for n should not diverge faster than $n = 4$ to maintain our CHDE model subdominant in these Universe's eras, only becoming dominant at later times, $z < 1$.

Eq. (2.4) evaluated at present, $\eta = \eta_0$, imposes a constraint on the DE,

$$1 = \Omega_b^{(0)} + \Omega_\gamma^{(0)} + \Omega_{dm}^{(0)} + \Omega_{\mathcal{M}}^{(0)}. \quad (2.6)$$

The new complexity is that this constraint demands computing $H_0\eta_0$, so we implemented the check of this constraint, complying it at every time step.

3 Model testing with cosmological data

We modified the code `class` [22] according to our model, see equations in Appendix B, and performed the parameter inference computations using the code `Cobaya` [23]. We carried out a Markov Chain Monte Carlo (MCMC) bayesian likelihood function fitting to different datasets: DESI BAO DR2 [4] (for short, BAO), Planck CMB full multipoles using the Planck PR4 `CamSpec` likelihood [24, 25], the Atacama Cosmology Telescope (ACT) lensing data [26–28], and supernovae compilations (dubbed SNIa data): Pantheon+ [7], Union3 [29], and DES Year 5 [10]. This whole set of data are described in more detail in refs. [1, 4].

To understand the role of the new DE model, we performed different parameter inferences, one with fixed massive neutrinos to 0.06 eV (a single massive and two massless neutrinos) and the other with $\sum m_\nu$ as a free parameter. We also run inferences for a flat Universe and for curvature as a free parameter (again with a single massive neutrino). The inclusion of massive neutrinos and curvature as free parameters is motivated by the recent debate regarding the negative mass posterior probability [15, 30, 31] and curvature as a possible solution to this issue [16]. In particular, we consider the following set of data and models for the analysis:

A) Individual data of DESI BAO DR2, Planck, Pantheon+, DESY5, and Union3. For these datasets, we perform the inference allowing spatial curvature to vary while keeping the neutrino mass fixed, since when treated as a free parameter it is better constrained with the ACT lensing information that will be included in the subsequent datasets. Results of this set are in Table 2.

B) DESI BAO DR2 + SNIa for a model with free curvature and fixed neutrino mass, as in A, but now we use two datasets for the inference. Results of this set are in Table 3.

C) DESI BAO DR2 + Planck data + SNIa for a model with free curvature and fixed neutrino mass, as in A, but now we use three datasets for the inference. Results of this set are in Table 4.

D) DESI BAO DR2 + Planck + ACT for both curvature and neutrino mass as free parameters. Results of this set are in Table 5.

E) DESI BAO DR2 + Planck + ACT for a flat model and free neutrino parameter. Results of this set are in Table 6.

We opted to use the same priors as in the DESI BAO DR2 cosmological analysis [4] in order to compare their results for Λ CDM model with ours for the CHDE model. Our priors are displayed in Table 1, where we also vary the CHDE exponent n , see eq. (2.3). The CHDE strength parameter Q (or $\Omega_{\mathcal{M}}^{(0)}$) is a derived parameter obtained from the constraint equation (2.6), similar as it happens in the Λ CDM model to determine Ω_Λ .

The inferred cosmological parameters are summarized in the following tables and figures. Our results report best-fitted parameters with 68% confidence levels (C.L.), except for $\sum m_\nu$ for which we report 95% C.L. Table 2 presents the results obtained for data set A. Independent analyzes of BAO and SNIa allow for a relatively broad range of parameter values within our model, indicating that the CHDE scenario remains partially consistent with the standard Λ CDM model, which is recovered for the specific parameter choices ($\Omega_{\mathcal{M}}^{(0)} = \Omega_\Lambda, n = 0$). However, results from Planck data alone exclude Λ CDM. Also, the joint analysis of BAO and SNIa displayed in Table 3 points to the discarding of the Λ CDM model. Next, Table 4 reports the parameter constraints derived from the combined BAO+Planck+SNIa data. In this case, the Λ CDM model is disfavored with even greater statistical precision: the nonflat

Parameters	Priors
n	$\mathcal{U}(-1, 1)$
Ω_K	$\mathcal{U}(-0.3, 0.3)$
H_0 [km/s/Mpc]	$\mathcal{U}(20, 100)$
ω_b	$\mathcal{G}(0.0222, 0.0005^2)$
ω_{cdm}	$\mathcal{U}(0.001, 0.99)$
$\ln(10^{10} A_s)$	$\mathcal{U}(1.61, 3.91)$
n_s	$\mathcal{U}(0.8, 1.2)$
τ_{reio}	$\mathcal{U}(0.01, 0.8)$
$\sum m_\nu$ [eV]	$\mathcal{U}(0, 5)$

Table 1. Priors of the relevant fitting parameters. \mathcal{U} y \mathcal{G} make reference to flat and uninformative priors, respectively.

model is discarded by 4.4σ , whereas the flat model is 4.5σ away from Λ CDM. These results are presented more visually in Figure 1, which shows contour plots for the best-fitted parameters of the model $(\Omega_{\mathcal{M}}^{(0)}, n)$ for the analysis combining the different sets. The joint analysis clearly discards the Λ CDM model (dashed lines).

As it happens in the Λ CDM model, Ω_m is smaller for BAO than for Planck, but the discrepancy is larger in our CHDE model. Figure 2 shows the matter density parameter vs the Hubble constant (left panel) and 1-dimensional (1D) marginalized posteriors when using different datasets (right panel). Also in this figure one observes a shift in the value of the Hubble constant towards larger values than in Λ CDM (vertical dashed line). The reported value in Table 4 for BAO-Planck-Pantheon+ data is $H_0 = 70.75_{-1.2}^{+0.81}$ h/Mpc when Ω_k is a free parameter, whereas in Λ CDM is 63.3 ± 2.1 h/Mpc [4]. For a flat cosmology, we report in Table 6 a value of 67.40 ± 0.36 h/Mpc and Λ CDM for Planck data is 67.36 ± 0.54 h/Mpc [32], that are compatible values to 1σ . These results are shown in Figure 3. Thus, the results for H_0 do not solve the Hubble tension using early universe physics (CMB and BAO).

With runs A-D we explore the role of curvature in our CHDE model. The curvature behaves similar to the Λ CDM model's: Planck fitting results in a small negative Ω_k [25], whereas for DESI BAO fitting it is positive [4], thought in our case Ω_k is larger with larger uncertainties too, since we have an extra parameter. These results are shown in Table 2, and Figure 4 shows the contour plots of the curvature vs the matter parameter. Further fittings that include BAO data in Tables 3-5 show a preference for a positive Ω_k .

In recent determinations of the summed neutrino mass ($\sum m_\nu$), the DESI collaboration reports very small values that may eventually come into tension with terrestrial oscillation experiments, which establish a lower bound on this quantity of $\sum m_\nu > 0.059$ eV for normal mass hierarchy (NH) and $\sum m_\nu > 0.1$ eV for inverted hierarchy (IH) [33]. The result found in the DESI DR2 analysis is, for a flat cosmology, $\sum m_\nu < 0.0642$ eV (95% C.L.) [4], and SPT-3G D1+DESI and CMB-SPA+DESI combinations appear to rule out the normal and inverted hierarchies at 97.9% and 99.9% confidence, respectively [34]. Furthermore, the maximum posterior probability lies at nonphysical, negative values [15]. These conflicting results open

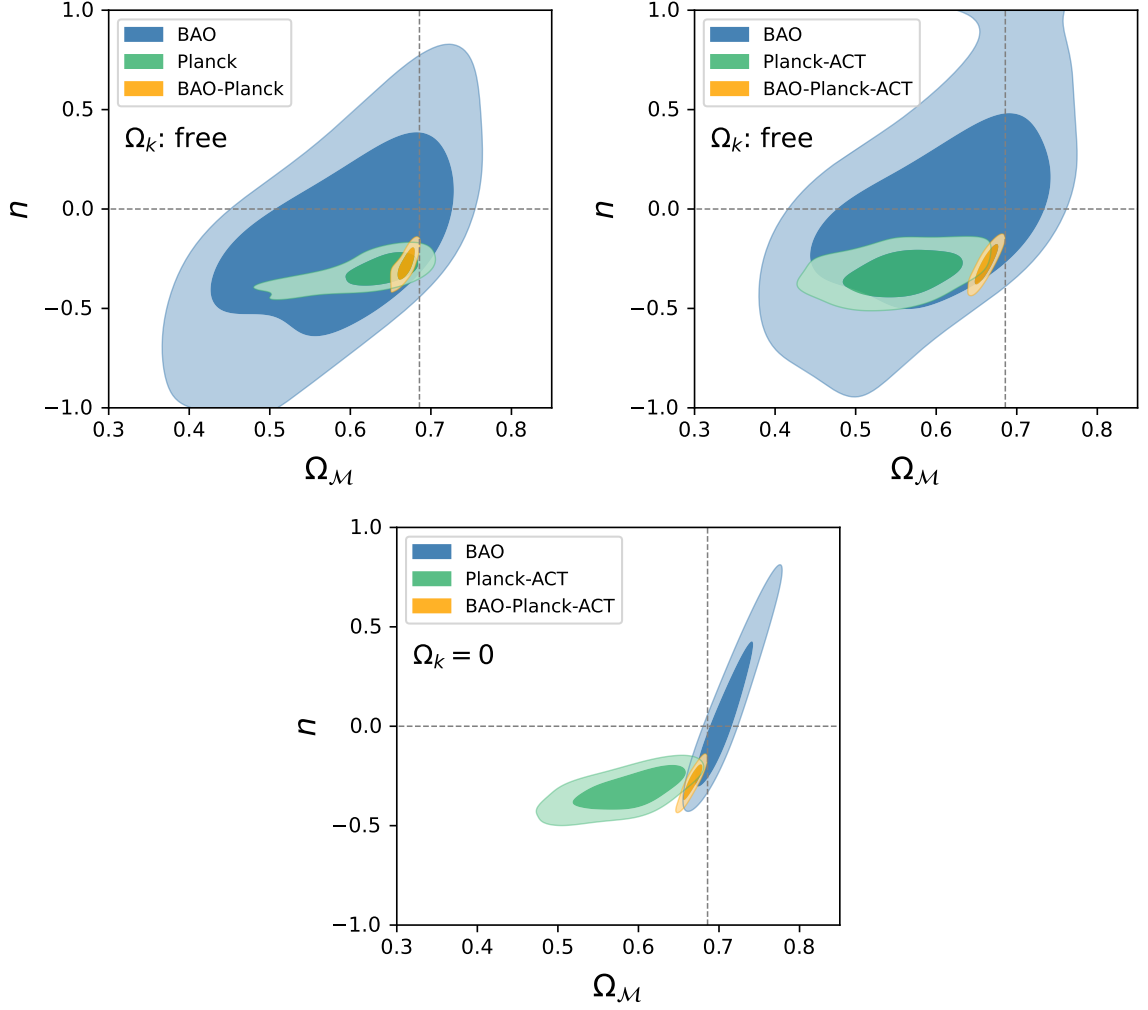


Figure 1. Contours plots of the CHDE model parameters: the density parameter of DE ($\Omega_{\mathcal{M}}^{(0)}$) and the power law exponent (n), cf. eq. (2.3). The cosmological parameters and data of each plot are combination of the different sets: the left panel correspond to results of BAO and Planck with the curvature as free parameter; the right panel corresponds to BAO, Planck, and ACT, also for free curvature; and the panel below corresponds to BAO, Planck, and ACT for a flat model. Our results exclude the Λ CDM model ($\Omega_{\mathcal{M}}^{(0)} = \Omega_{\Lambda}$, $n = 0$, dashed lines) as a best fit when CMB data are included.

the possibility for alternative scenarios. In this sense, reference [16] argues that inclusion of the curvature as free parameter relaxes the constraint to $\sum m_{\nu} < 0.1$ eV (95% C.L.) and making the posterior probability more positive, thus hinting to have solved the problem. However, their maximum probability is around zero, suggesting that a full resolution would imply to perform an analysis with effective negative neutrino masses [15]. In our CHDE model we computed the neutrino mass, using sets D (free curvature) and E (flat model), obtaining the results in Tables 5 and 6: we obtain $\sum m_{\nu} = 0.34^{+0.34}_{-0.30}$ eV (95% C.L.) with a negative Ω_k when using Planck+ACT data and $\sum m_{\nu} = 0.037^{+0.070}_{-0.052}$ eV (95% C.L.) with BAO+Planck+ACT data resulting a positive Ω_k as in ref. [16]. For a flat cosmology, we obtain $\sum m_{\nu} = 0.39^{+0.46}_{-0.39}$ eV (95% C.L.) when using Planck+ACT data and $\sum m_{\nu} = 0.021^{+0.040}_{-0.029}$ eV

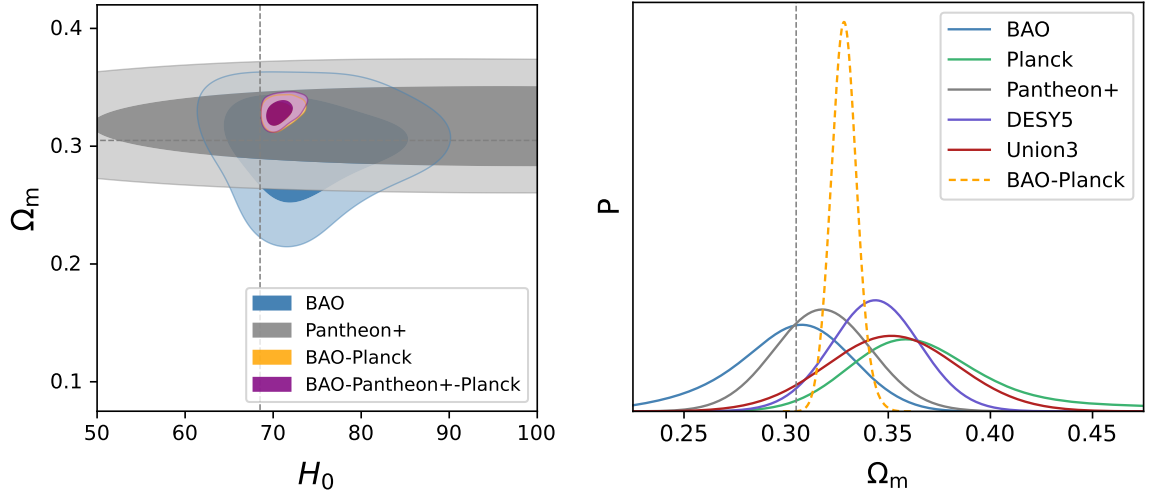


Figure 2. Contours plots of matter density parameter vs the Hubble constant for the CHDE model (left) and the marginalized 1D posteriors probabilities (P) for different datasets. As a reference, the black dashed line points to the best fit values for the Λ CDM model using Planck data.

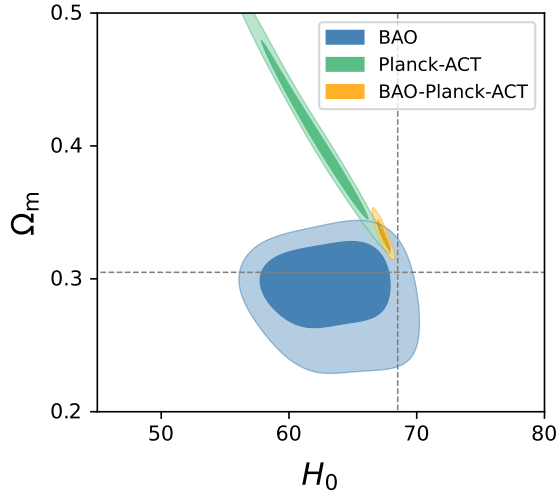


Figure 3. Contours plots of matter density parameter vs the Hubble constant for the flat CHDE model. As a reference, the black dashed line points to the best fit values for the Λ CDM model using Planck data.

(95% C.L.) with BAO+Planck+ACT data. Both results are compatible with the terrestrial oscillation experiment results within 95% C.L. Furthermore, Figure 5 depicts the marginalized 1D posterior probabilities for nonflat and flat models, clearly shown that the maximum for both cases lies in the positive values for the CHDE model. As we mentioned, DESI data determined a lower Ω_m than Planck data and this fact reduces the convergence of $\sum m_\nu$ when these datasets are combined. Figure 6 shows these results for flat and non-flat models,

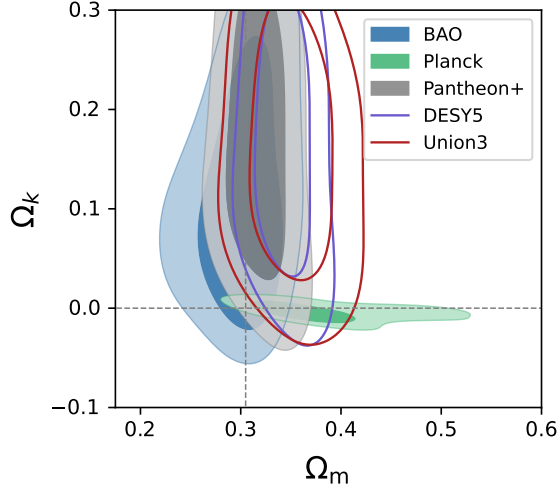


Figure 4. Contours plots of the curvature and matter density parameters for the CHDE model.

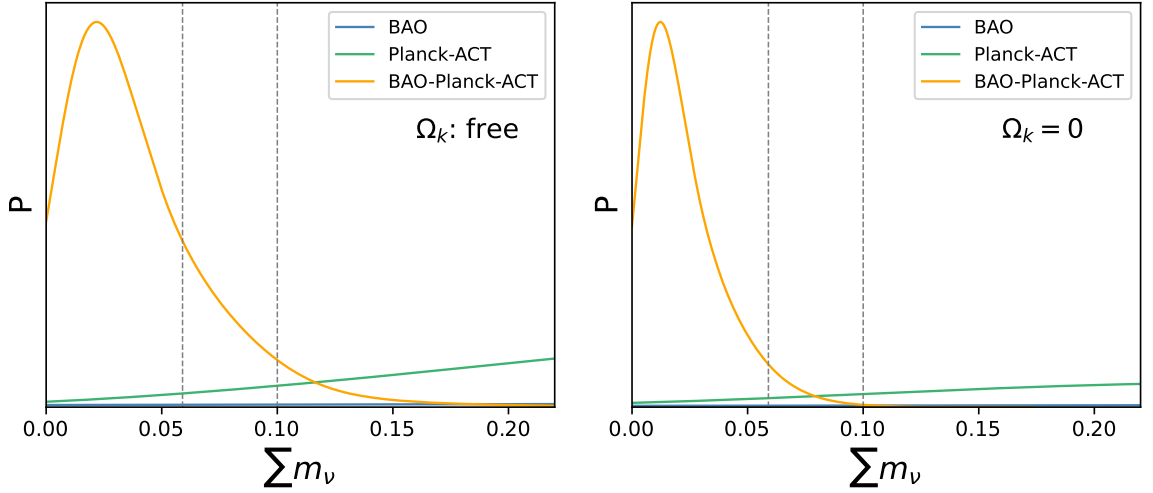


Figure 5. Posterior probabilities of the sum of the neutrino masses for nonflat (left panel) and flat (right panel) models for the CHDE model. Both plots show a maximum probability in the positive neutrino masses. For reference vertical dashed lines indicate the NH and IH experimental limits from terrestrial experiments, at 0.059 eV and 0.1 eV, respectively.

in which one can see that the concordance zone, where probabilities coincide, is small, resulting in a small $\sum m_\nu$.

In appendix C we show the contour plots of a larger set of relevant cosmological parameters of the different runs. Figure 7 shows results from set C with a free curvature model and fixed neutrino mass; Figure 8 shows results from set D with a free curvature model and free neutrino mass; Figure 8 shows results from sets E for flat model with a free neutrino mass.

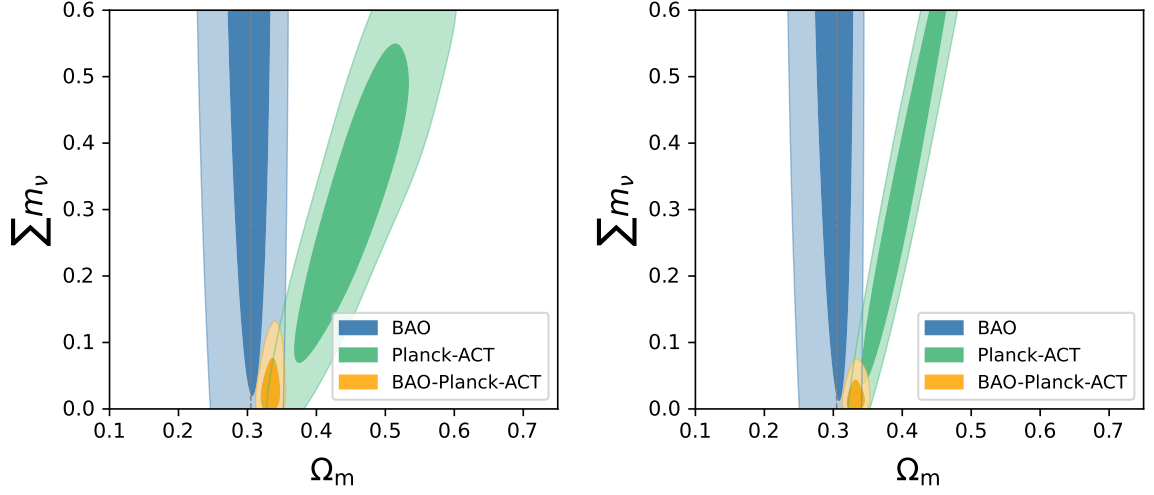


Figure 6. Contours plots of the neutrino mass vs the matter density parameter. Left panel is for Ω_k as a free parameter and right panel for a flat model. The region of concordance in the joint analysis is quite narrow, driving the inferred neutrino mass towards very small values.

	BAO	Planck	Pantheon+	DESY5	Union3
Parameter	68% limits	68% limits	68% limits	68% limits	68% limits
n	$-0.15^{+0.31}_{-0.37}$	-0.312 ± 0.056	$-0.28^{+0.30}_{-0.49}$	$-0.41^{+0.22}_{-0.50}$	$-0.40^{+0.18}_{-0.55}$
Ω_k	$0.107^{+0.069}_{-0.10}$	$-0.0041^{+0.0060}_{-0.0068}$	$0.149^{+0.11}_{-0.077}$	$0.151^{+0.10}_{-0.075}$	$0.148^{+0.098}_{-0.078}$
$\Omega_b h^2$	0.02222 ± 0.00050	$0.02226^{+0.00041}_{-0.00017}$	0.02222 ± 0.00050	0.02222 ± 0.00050	0.02223 ± 0.00050
Ω_m	$0.302^{+0.033}_{-0.025}$	$0.374^{+0.023}_{-0.048}$	0.318 ± 0.024	0.344 ± 0.022	0.352 ± 0.032
$H_0[\text{km/s/Mpc}]$	$73.7^{+4.6}_{-7.5}$	66.7 ± 3.5	108^{+40}_{-40}	109^{+40}_{-40}	109^{+40}_{-40}
$\Omega_{\mathcal{M}}$	$0.592^{+0.12}_{-0.073}$	$0.630^{+0.045}_{-0.019}$	0.533 ± 0.084	0.505 ± 0.082	$0.500^{+0.085}_{-0.094}$

Table 2. Parameter inference for the relevant cosmological parameters using independent BAO DESI DR2, Planck, and SNIa data. Results from set A explained in the main text.

	BAO-Pantheon+	BAO-DESY5	BAO-Union3
Parameter	68% limits	68% limits	68% limits
n	-0.30 ± 0.24	-0.52 ± 0.24	-0.44 ± 0.28
Ω_k	$0.129^{+0.080}_{-0.10}$	0.156 ± 0.078	0.146 ± 0.081
$\Omega_b h^2$	0.02222 ± 0.00050	0.02223 ± 0.00050	0.02223 ± 0.00050
Ω_m	0.314 ± 0.019	0.332 ± 0.017	0.326 ± 0.021
$H_0[\text{km/s/Mpc}]$	$75.0^{+6.2}_{-7.9}$	$74.3^{+6.9}_{-8.0}$	$74.4^{+6.7}_{-8.0}$
$\Omega_{\mathcal{M}}$	$0.556^{+0.10}_{-0.073}$	0.511 ± 0.081	0.528 ± 0.086

Table 3. Results for the joint analysis of BAO DR2 + SNIa data. Results from set B.

	BAO-Pantheon+-Planck	BAO-DES5-Planck	BAO-Union3-Planck
Parameter	68% limits	68% limits	68% limits
n	-0.285 ± 0.061	-0.284 ± 0.052	-0.280 ± 0.054
Ω_k	$0.0027^{+0.0016}_{-0.0033}$	$0.0021^{+0.0015}_{-0.0024}$	$0.0023^{+0.0016}_{-0.0024}$
$\Omega_b h^2$	$0.02250^{+0.00018}_{-0.00015}$	0.02249 ± 0.00016	0.02248 ± 0.00016
Ω_m	$0.3295^{+0.0066}_{-0.0076}$	0.3304 ± 0.0063	$0.3296^{+0.0062}_{-0.0070}$
$H_0[\text{km/s/Mpc}]$	$70.75^{+0.81}_{-1.2}$	$70.43^{+0.74}_{-0.85}$	$70.43^{+0.70}_{-0.87}$
$\Omega_{\mathcal{M}}$	$0.6678^{+0.0096}_{-0.0068}$	$0.6674^{+0.0074}_{-0.0063}$	$0.6680^{+0.0081}_{-0.0064}$

Table 4. Results for the joint analysis employing BAO DR2+Planck+SNIa data. Results from set C.

	Planck-ACT	BAO-Planck-ACT
Parameter	68% limits	68% limits
n	-0.321 ± 0.080	-0.279 ± 0.064
Ω_k	-0.0176 ± 0.0079	$0.0038^{+0.0017}_{-0.0022}$
$\Omega_b h^2$	0.02215 ± 0.00016	0.02220 ± 0.00013
Ω_m	$0.462^{+0.050}_{-0.059}$	0.3344 ± 0.0086
$H_0[\text{km/s/Mpc}]$	57.8 ± 3.4	67.68 ± 0.39
$\Omega_{\mathcal{M}}$	$0.556^{+0.052}_{-0.044}$	0.6618 ± 0.0096
$\sum m_\nu[\text{eV}] (95\% \text{ C.L.})$	$0.34^{+0.34}_{-0.30}$	$0.037^{+0.070}_{-0.052}$

Table 5. Results for the joint analysis employing Planck+ACT DR6 and BAO DR2+Planck+ACT DR6 data for a non-flat model. Neutrino masses are given in eV and reported with 95% C.L., as standard. Results from set D.

	Planck-ACT	BAO-Planck-ACT
Parameter	68% limits	68% limits
n	-0.322 ± 0.074	$-0.279^{+0.065}_{-0.052}$
$\Omega_b h^2$	$0.02196^{+0.00021}_{-0.00017}$	0.02233 ± 0.00012
Ω_m	$0.412^{+0.036}_{-0.054}$	$0.3327^{+0.0073}_{-0.0086}$
$H_0[\text{km/s/Mpc}]$	$61.9^{+3.3}_{-2.4}$	67.40 ± 0.36
$\Omega_{\mathcal{M}}$	$0.588^{+0.054}_{-0.036}$	$0.6672^{+0.0086}_{-0.0073}$
$\sum m_\nu[\text{eV}] (95\% \text{ C.L.})$	$0.39^{+0.46}_{-0.39}$	$0.021^{+0.040}_{-0.029}$

Table 6. Results for the joint analysis employing Planck+ACT DR6 and BAO DR2+Planck+ACT DR6 data for a flat model. Neutrino masses are given in eV and reported with 95% C.L., as standard. Results from set E.

4 Conclusions

The striking recent results put forward by the DESI collaboration [1, 4] that suggest an evolving DE component, instead of a constant, motivate us and many colleagues to test other possible models for background expansion. Furthermore, notable discrepancies were identified in the inferred values of the matter density parameter, for which DESI yields a lower value, while Planck favors a higher one. Also, the neutrino mass determined by DESI seems to be within the limit of the permitted values from oscillation experiments, and its resulting posterior lies on the negative mass side.

As an alternative to Λ CDM, we propose a model, a holographic model, dubbed CHDE, that depends on the conformal time, with an exponent (n), which can be determined by observations; this represents an extra parameter with respect to the Λ CDM model. The model differs from the standard holographic formulation but resembles the vacuum dark energy model [13]; its equation of state is $w_{DE} = -1$, but it includes an interaction with dark energy through the horizon term. We have tested the model using different datasets of BAO and SNIa distances and CMB spectra, which were also employed by the DESI collaboration in their recent results. We divided our parameter inference runs into different sets (A-E) to address different questions. First of all, our model theoretically includes the Λ CDM model for the case $n = 0$. Our results, however, demonstrate that Λ CDM is not favored as a best fit when using CMB data alone or in joint analysis with BAO and SNIa data. Tables 4-6 show consistent results for flat and nonflat models separately: Using Planck+ACT data alone results in $n \sim -0.32 \pm 0.1$ and using BAO+Planck+SNIa and BAO+Planck+ACT predicts approximately $n \sim -0.28 \pm 0.1$. A negative n implies, from eq. (2.5), a positive source of matter production, implying that our CHDE model is in fact a model with dark energy density that increases with time until the time η_0 but eventually decays following the power law, eq. (2.3).

As it happens in Λ CDM, the CHDE model tends to have a lower Ω_m with DESI data than the one obtained with Planck data, and this fact plays a role in the determination of the neutrino mass, as shown in Figure 6. This leads to a small neutrino mass, similar to what occurs in the flat Λ CDM model. We computed the neutrino mass in both flat and free-curvature scenarios using different datasets, and in all cases our constraints remain compatible with results from terrestrial oscillation experiments. Moreover, the posterior distributions exhibit a maximum at positive values of $\sum m_\nu$, thereby avoiding the issue present in the Λ CDM model, where the probability peaks on the negative side.

Acknowledgments

The authors thank Hernán E. Noriega for helpful comments on the neutrino section and acknowledge support by SECIHTI project CBF2023-2024-589. MARM acknowledges that the results and analysis of MCMC chains in this work used the DiRAC@Durham facility managed by the Institute for Computational Cosmology on behalf of the STFC DiRAC HPC Facility (www.dirac.ac.uk). The equipment was funded by BEIS capital funding via STFC capital grants ST/K00042X/1, ST/P002293/1, ST/R002371/1 and ST/S002502/1, Durham University and STFC operations grant ST/R000832/1. DiRAC is part of the National e-Infrastructure in the U.K.

References

- [1] DESI collaboration, A. G. Adame et al.,
DESI 2024 VI: cosmological constraints from the measurements of baryon acoustic oscillations,
[JCAP](#) **02** (2025) 021, [[2404.03002](#)].
- [2] DESI collaboration, R. Calderon et al.,
DESI 2024: reconstructing dark energy using crossing statistics with DESI DR1 BAO data,
[JCAP](#) **10** (2024) 048, [[2405.04216](#)].
- [3] DESI collaboration, K. Lodha et al.,
DESI 2024: Constraints on physics-focused aspects of dark energy using DESI DR1 BAO data,
[Phys. Rev. D](#) **111** (2025) 023532, [[2405.13588](#)].

- [4] DESI collaboration, M. A. Karim et al.,
DESI DR2 Results II: Measurements of Baryon Acoustic Oscillations and Cosmological Constraints, [2503.14738](#).
- [5] DESI collaboration, K. Lodha et al.,
Extended Dark Energy analysis using DESI DR2 BAO measurements, [2503.14743](#).
- [6] DES collaboration, T. M. C. Abbott et al.,
Dark Energy Survey: implications for cosmological expansion models from the final DES Baryon Acoustic Oscillations, [2503.06712](#).
- [7] D. Scolnic et al., The Pantheon+ Analysis: The Full Data Set and Light-curve Release, [Astrophys. J. **938** \(2022\) 113](#), [[2112.03863](#)].
- [8] D. Brout et al., The Pantheon+ Analysis: Cosmological Constraints, [Astrophys. J. **938** \(2022\) 110](#), [[2202.04077](#)].
- [9] D. Rubin et al.,
Union Through UNITY: Cosmology with 2,000 SNe Using a Unified Bayesian Framework, [2311.12098](#).
- [10] DES collaboration, T. M. C. Abbott et al.,
The Dark Energy Survey: Cosmology Results with ~ 1500 New High-redshift Type Ia Supernovae Using the Full Dataset, [Astrophys. J. Lett. **973** \(2024\) L14](#), [[2401.02929](#)].
- [11] S. Wang, Y. Wang and M. Li, Holographic Dark Energy, [Phys. Rept. **696** \(2017\) 1–57](#), [[1612.00345](#)].
- [12] H. Wei and R.-G. Cai, A New Model of Agegraphic Dark Energy, [Phys. Lett. B **660** \(2008\) 113–117](#), [[0708.0884](#)].
- [13] D. Wands, J. De-Santiago and Y. Wang, Inhomogeneous vacuum energy, [Class. Quant. Grav. **29** \(2012\) 145017](#), [[1203.6776](#)].
- [14] J. De-Santiago, D. Wands and Y. Wang, Inhomogeneous and interacting vacuum energy, in 6th International Meeting on Gravitation and Cosmology, 9, 2012. [1209.0563](#).
- [15] DESI collaboration, W. Elbers et al.,
Constraints on Neutrino Physics from DESI DR2 BAO and DR1 Full Shape, [2503.14744](#).
- [16] S.-F. Chen and M. Zaldarriaga, It's all Ok: curvature in light of BAO from DESI DR2, [JCAP **08** \(2025\) 014](#), [[2505.00659](#)].
- [17] M. Chevallier and D. Polarski, Accelerating universes with scaling dark matter, [Int. J. Mod. Phys. D **10** \(2001\) 213–224](#), [[gr-qc/0009008](#)].
- [18] E. V. Linder, Exploring the expansion history of the universe, [Phys. Rev. Lett. **90** \(2003\) 091301](#), [[astro-ph/0208512](#)].
- [19] T. Matos, L. A. Escamilla, M. Hernández-Marquez and J. A. Vázquez,
Cosmology on a gravitational wave background, [Mon. Not. Roy. Astron. Soc. **529** \(2024\) 3013–3019](#), [[2309.09989](#)].
- [20] T. Matos and L. L-Parrilla, The graviton Compton mass as Dark Energy, [Rev. Mex. Fis. **67** \(2021\) 040703](#), [[2108.05206](#)].
- [21] D. Blas, J. Lesgourgues and T. Tram,
The Cosmic Linear Anisotropy Solving System (CLASS) II: Approximation schemes, [JCAP **07** \(2011\) 034](#), [[1104.2933](#)].
- [22] D. Blas, J. Lesgourgues and T. Tram, The cosmic linear anisotropy solving system (class). part ii: Approximation schemes, [Journal of Cosmology and Astroparticle Physics **2011** \(July, 2011\) 034–034](#).

- [23] J. Torrado and A. Lewis, Cobaya: Code for Bayesian Analysis of hierarchical physical models, [JCAP](#) **05** (2021) 057, [[2005.05290](#)].
- [24] G. Efstathiou and S. Gratton, A Detailed Description of the CamSpec Likelihood Pipeline and a Reanalysis of the Planck High Frequency Maps, [MNRAS](#) **491** (2020) 1910.00483.
- [25] E. Rosenberg, S. Gratton and G. Efstathiou, CMB power spectra and cosmological parameters from Planck PR4 with CamSpec, [Mon. Not. Roy. Astron. Soc.](#) **517** (2022) 4620–4636, [[2205.10869](#)].
- [26] ACT collaboration, M. S. Madhavacheril et al., The Atacama Cosmology Telescope: DR6 Gravitational Lensing Map and Cosmological Parameters, [Astrophys. J.](#) **962** (2024) 113, [[2304.05203](#)].
- [27] ACT collaboration, F. J. Qu et al., The Atacama Cosmology Telescope: A Measurement of the DR6 CMB Lensing Power Spectrum and Its Implications, [Astrophys. J.](#) **962** (2024) 112, [[2304.05202](#)].
- [28] ACT collaboration, N. MacCrann et al., The Atacama Cosmology Telescope: Mitigating the Impact of Extragalactic Foregrounds for the DR6 Cosmic Microwave Background, [Astrophys. J.](#) **966** (2024) 138, [[2304.05196](#)].
- [29] D. Rubin et al., Union Through UNITY: Cosmology with 2,000 SNe Using a Unified Bayesian Framework, [MNRAS](#) **478** (2018) 2311.12098.
- [30] N. Craig, D. Green, J. Meyers and S. Rajendran, No ν_s is Good News, [JHEP](#) **09** (2024) 097, [[2405.00836](#)].
- [31] W. Elbers, C. S. Frenk, A. Jenkins, B. Li and S. Pascoli, Negative neutrino masses as a mirage of dark energy, [Phys. Rev. D](#) **111** (2025) 063534, [[2407.10965](#)].
- [32] PLANCK collaboration, N. Aghanim et al., Planck 2018 results. VI. Cosmological parameters, [Astron. Astrophys.](#) **641** (2020) A6, [[1807.06209](#)].
- [33] I. Esteban, M. C. Gonzalez-Garcia, M. Maltoni, I. Martinez-Soler, J. P. Pinheiro and T. Schwetz, NuFit-6.0: updated global analysis of three-flavor neutrino oscillations, [JHEP](#) **12** (2024) 216, [[2410.05380](#)].
- [34] SPT-3G collaboration, E. Camphuis et al., SPT-3G D1: CMB temperature and polarization power spectra and cosmology from 2019 and 2020 observations, [MNRAS](#) **506** (2021) 2506.20707.
- [35] M. Maggiore, Gravitational wave experiments and early universe cosmology, [Phys. Rept.](#) **331** (2000) 283–367, [[gr-qc/9909001](#)].

A Alternative interpretation of the CHDE model

The main idea is to take into account the energy of the primordial gravitational waves of the universe instead of the cosmological constant. For this purpose, it is well known that the contribution of the Gravitational Wave Background (GWB) density rate Ω_{GWB} to the universe is given by [35]:

$$\Omega_{GWB} = \frac{2\pi^2 f^2}{3H_0^2} h_c^2. \quad (\text{A.1})$$

Here h_c is the dimensionless characteristic amplitude representing a characteristic value of the amplitude per unit logarithmic interval of frequency f and H_0 is the current value of the

Hubble parameter. Instead of the frequency we can consider the wavelength ($\lambda = c/f$):

$$h_c(f) = A \left(\frac{f}{f_*} \right)^\alpha = A \left(\frac{\lambda_*}{\lambda} \right)^\alpha. \quad (\text{A.2})$$

Eq. (A.1) can be written in the following form

$$\Omega_{GWB} = \mathcal{M} h_c^2 \frac{c^2}{3H_0^2} \quad (\text{A.3})$$

where \mathcal{M} is related to the graviton wavelength as

$$\mathcal{M} = \frac{2\pi^2}{\lambda^2}. \quad (\text{A.4})$$

λ is the wavelength of the primordial gravitational waves that propagate at the speed of light which means that

$$\lambda = c \int \frac{dt}{a} = \eta \quad (\text{A.5})$$

being a the scale factor of the universe and η the conformal time; see [20] for an alternative derivation of the above formulae.

Observe that then $\mathcal{M} h_c^2$ can be written as Eq. (2.2):

$$\mathcal{M} h_c^2 = \frac{2\pi^2}{\lambda^2} A \left(\frac{\lambda_*}{\lambda} \right)^\alpha = B \lambda^n \quad (\text{A.6})$$

where $B = 2\pi^2 A \lambda_*^\alpha$ and $n = -\alpha - 2$. In the main text, we propose this type of term gives rise to CHDE, and here we conjecture that this may come from a GW contribution, as argued in reference [20].

B Cosmological equations for class

`class` uses the number of e-folds ($N \equiv \ln a$) to evolve the equations, but at any time one can also make use the cosmic time (t) or conformal time (η). Since our CHDE model is given in terms of the conformal time, we write first order cosmological equations as (with units $\frac{8\pi G}{3} = 1$):

$$\frac{d\rho_m}{dN} = -3\rho_m - \frac{nQ}{3a} \frac{H_0^3}{H} (H_0\eta)^{n-1}, \quad (\text{B.1})$$

$$\frac{dt}{dN} = \frac{1}{H}, \quad (\text{B.2})$$

$$\frac{d\eta}{dN} = \frac{1}{aH}, \quad (\text{B.3})$$

$$\frac{dr_s}{dN} = \frac{c_s}{aH}, \quad (\text{B.4})$$

$$\frac{dD}{dN} = \frac{D_p}{aH}, \quad (\text{B.5})$$

$$\frac{dD_p}{dN} = -D_p + \frac{3}{2} a \rho_m \frac{D}{H}, \quad (\text{B.6})$$

whereby

$$H^2 = \frac{\rho_b^{(0)}}{a^3} + \frac{\rho_\gamma^{(0)}}{a^4} + \rho_m + \frac{QH_0^2}{3}(H_0\eta)^n \quad (\text{B.7})$$

and the following definitions apply:

$$ad\eta \equiv dt, \text{ cosmic time} \quad (\text{B.8})$$

$$c_s \equiv \frac{1}{\sqrt{3\left(1 + \frac{3\rho_b}{4\rho_\gamma}\right)}}, \text{ plasma sound speed}, \quad (\text{B.9})$$

$$r_s \equiv \int_0^\eta d\eta' c_s(\eta'), \text{ sound horizon}, \quad (\text{B.10})$$

$$D \equiv \delta_m, \text{ matter density contrast}, \quad (\text{B.11})$$

$$D_p \equiv a H \frac{d\delta_m}{dN}. \quad (\text{B.12})$$

C Full contour plots of the CHDE model

As a reference, we present contour plots for a larger set of relevant parameters.

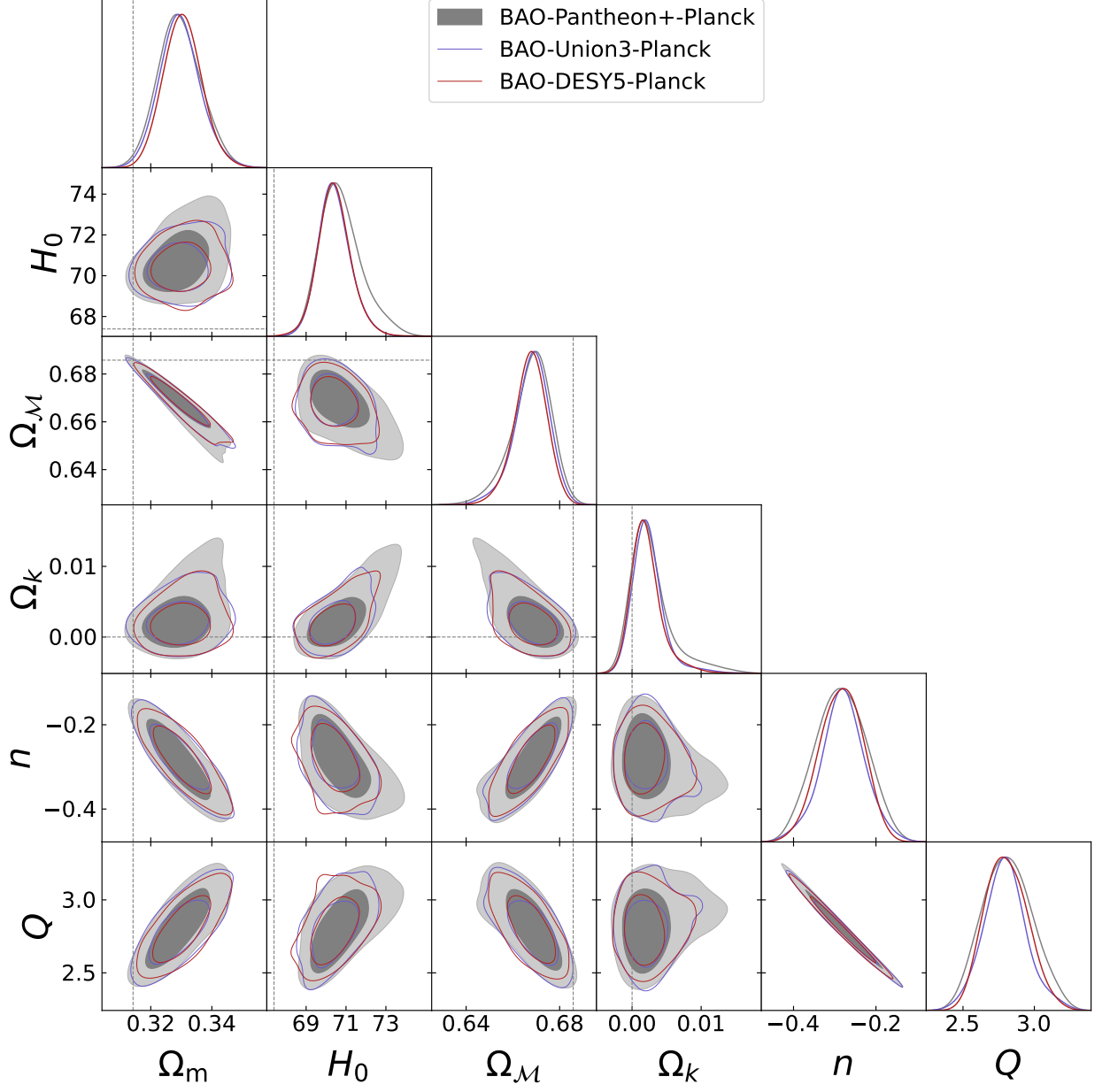


Figure 7. Contours plots of the relevant parameters for the CHDE model using set C with a free curvature model.

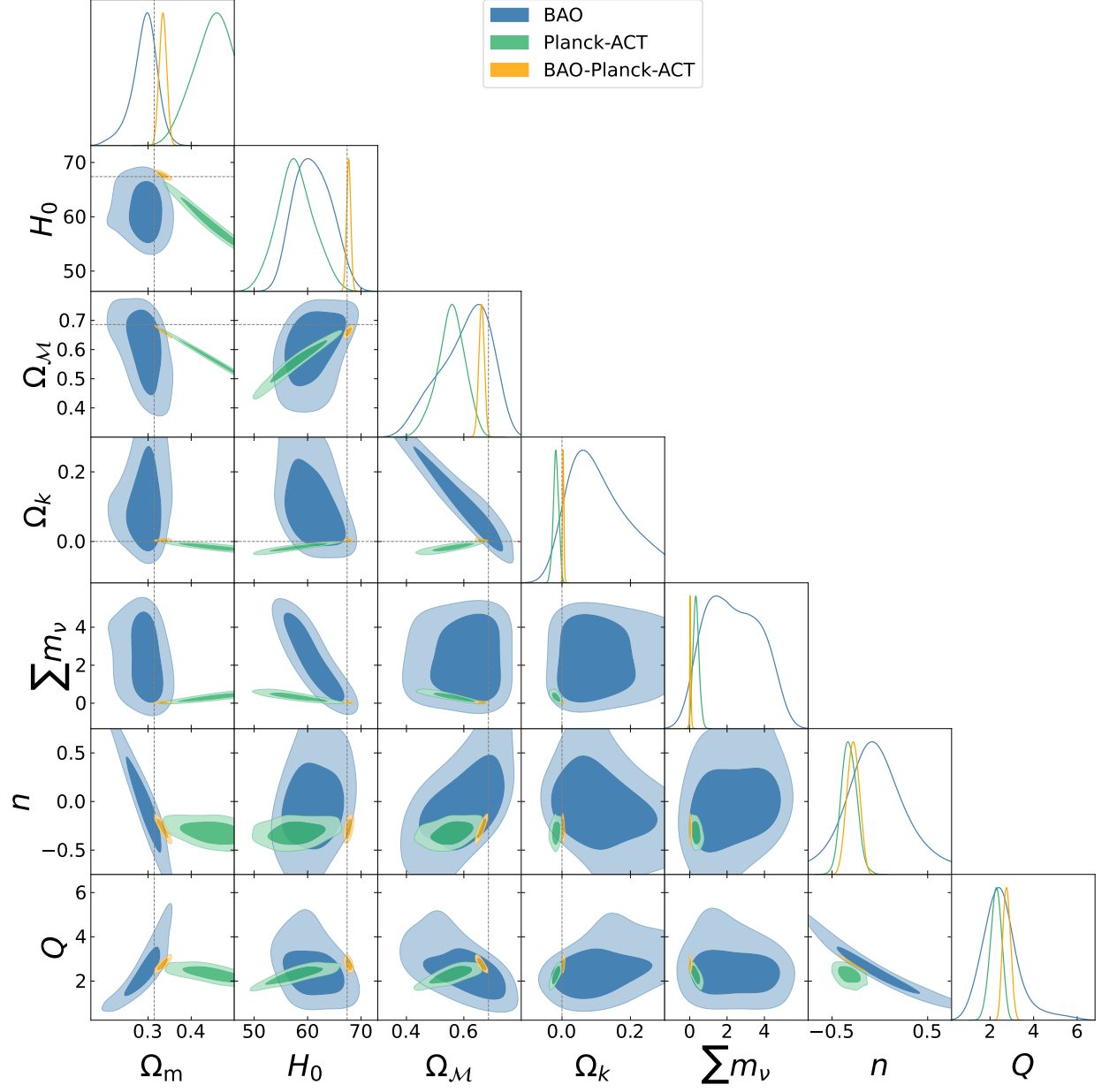


Figure 8. Contours plots of the relevant parameters for the CHDE model using set D with a free curvature model and free neutrino mass.

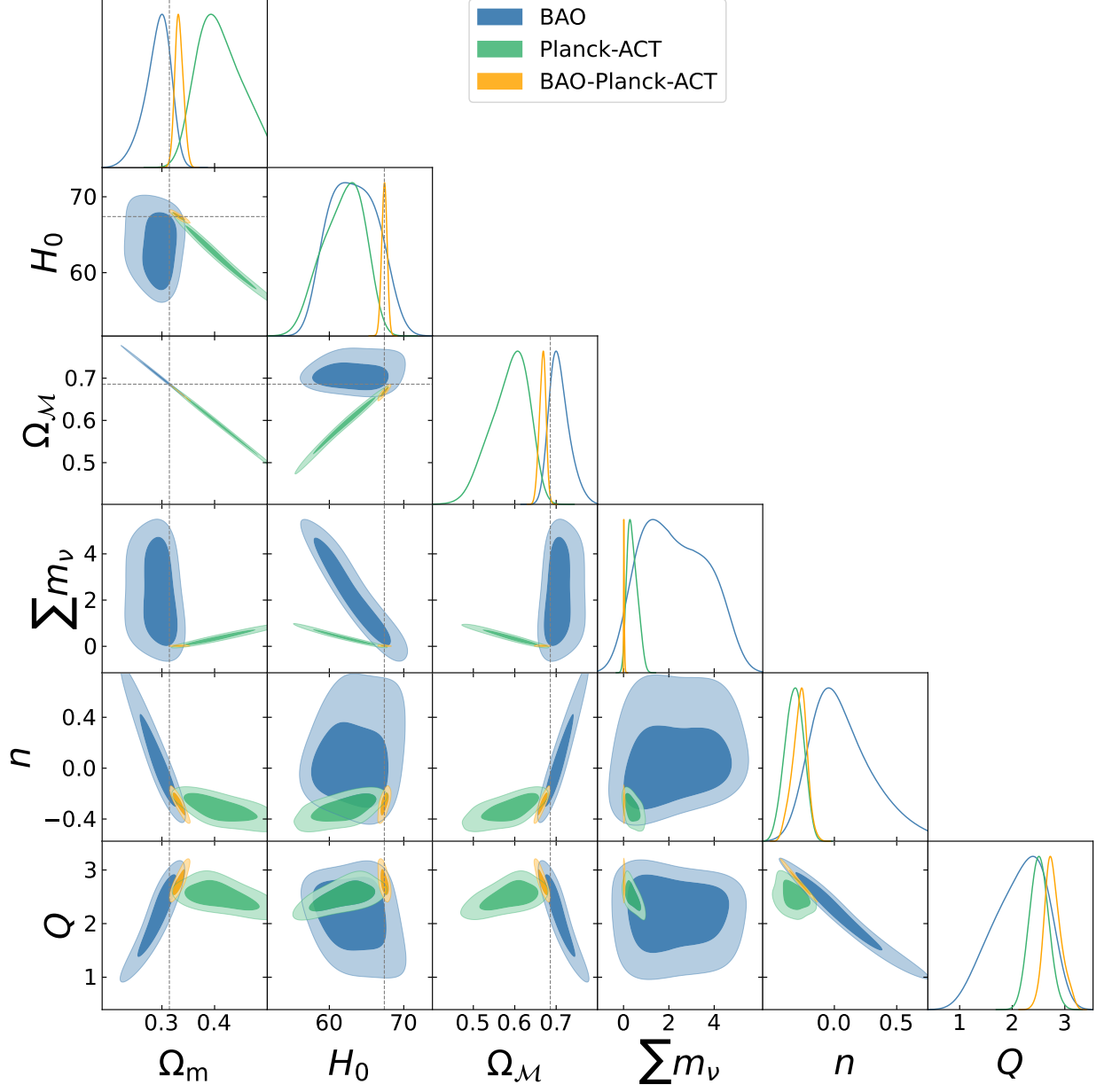


Figure 9. Contours plots of the relevant parameters for the CHDE model using set E for a flat model and free neutrino mass.